

Learning Where It Matters: Geometric Anchoring for Robust Preference Alignment

Youngjae Cho¹ Jongsuk Kim^{1,2} Ji-Hoon Kim¹

Abstract

Direct Preference Optimization (DPO) and related methods align large language models from pairwise preferences by regularizing updates against a fixed reference policy. As the policy drifts, a static reference, however, can become increasingly miscalibrated, leading to distributional mismatch and amplifying spurious preference signals under noisy supervision. Conversely, reference-free variants avoid mismatch but often suffer from unconstrained reward drift. We propose *Geometric Anchor Preference Optimization* (GAPO), which replaces the fixed reference with a dynamic, geometry-aware *anchor*: an adversarial local perturbation of the current policy within a small radius that serves as a pessimistic baseline. This anchor enables an adaptive reweighting mechanism, modulating the importance of each preference pair based on its local sensitivity. We further introduce the *Anchor Gap*, the reward discrepancy between the policy and its anchor, and show under smoothness conditions that it approximates worst-case local margin degradation. Optimizing a logistic objective weighted by this gap downweights geometrically brittle instances while emphasizing robust preference signals. Across diverse noise settings, GAPO consistently improves robustness while matching or improving performance on standard LLM alignment and reasoning benchmarks.

1. Introduction

Aligning large language models (LLMs) with human intent is a central problem in modern AI. While Reinforcement Learning from Human Feedback (RLHF) (Schulman et al., 2017; Ouyang et al., 2022; Christiano et al., 2017) has been the dominant paradigm, Direct Preference Optimization (DPO) (Rafailov et al., 2023) has emerged as a widely used alternative that learns directly from pairwise preferences.

¹PYLER ²KAIST. Correspondence to: Youngjae Cho <leon5760@gmail.com>.

DPO optimizes a logistic objective that is explicitly regularized against a fixed reference policy, enabling stable training without learning a separate reward model.

Despite its practical appeal, a fixed reference can become increasingly miscalibrated as the policy moves during optimization, raising distributional mismatch (Xiong et al., 2024; Meng et al., 2024). As the mismatch grows, the reference provides weaker guidance, yielding a poorly calibrated implicit preference signal (Azar et al., 2024). This in turn makes learning brittle under noisy supervision, encouraging the model to exploit spurious correlates of preference (e.g., style, verbosity) rather than robust semantic cues (Meng et al., 2024; Park et al., 2024).

Reference-free objectives such as SimPO (Meng et al., 2024) avoid explicit mismatch by defining rewards purely from the current policy’s likelihood. SimPO uses the length-normalized log probability as an implicit reward and enforces a target margin, leading to an efficient training pipeline. However, removing the reference also discards an explicit stabilizer, and the policy can over-optimize the implicit reward, resulting in unconstrained reward drift. Such drift can harm general capabilities (Lin et al., 2024; Noukhovitch et al., 2023) and exacerbate sensitivity to label noise (Chowdhury et al., 2024).

These trade-offs suggest a missing ingredient in offline preference optimization: a stabilizer that adapts as the policy evolves. We introduce *Geometric Anchor Preference Optimization* (GAPO), which stabilizes preference optimization by comparing the policy to a pessimistic local surrogate instead of a fixed reference. Concretely, GAPO constructs a pessimistic local surrogate by applying an adversarial (worst-case) perturbation to the current policy within a small radius. This anchor acts as a geometric stress test: if a preference signal remains consistent against a pessimistic neighbor, it is more likely to reflect robust semantics rather than fragile artifacts. Intuitively, spurious correlates of preference tend to be locally brittle, small distributional shifts can flip the preferred output, whereas semantically grounded preferences are more stable, which helps mitigate the impact of noisy supervision.

Based on this idea, we define the *Anchor Gap* as the dis-

crepancy between the policy’s implicit reward (likelihood-based) and the anchor’s implicit reward. We use this gap to adaptively reweight the logistic objective, downweighting instances that are geometrically brittle under perturbations while emphasizing stable preference signals.

On the theory side, we show that GAPO preserves the gradient direction of standard objectives (e.g., DPO, SimPO) up to an instance-wise scalar reweighting. Under mild smoothness assumptions, we prove that the Anchor Gap approximates the worst-case local margin degradation, providing a principled justification for geometric anchoring.

Empirically, GAPO matches or improves performance on standard instruction-following benchmarks and on more challenging reasoning and mathematical tasks. It also exhibits strong robustness under noisy preferences, including random label flips and systematic biases such as length-based spurious correlations.

Our contributions are as follows:

- We introduce *Geometric Anchor Preference Optimization* (GAPO), which stabilizes preference optimization via a pessimistic local surrogate (anchor) constructed around the current policy.
- We provide a theoretical guarantees showing that GAPO induces an instance-wise reweighting of gradients and that the Anchor Gap is connected to stability.
- We demonstrate that GAPO matches or exceeds strong baselines on instruction-following and reasoning benchmarks while substantially improving robustness to preference noise.

2. Related Work

Preference Optimization. Offline preference optimization is commonly formulated either (i) with an explicit *reference* policy that regularizes updates, or (ii) in a *reference-free* manner that trades off explicit stabilization for simplicity. DPO (Rafailov et al., 2023) is a representative reference-based objective, anchoring the policy to a fixed reference model to promote stable optimization. Building on this line, IPO (Azar et al., 2024) introduces a gap-regularized objective to mitigate overfitting, while KTO (Ethayarajh et al., 2024) leverages prospect theory to align models without paired preference data. To address practical issues such as length bias or weak supervision signals, variants such as RDPO (Park et al., 2024) and ORPO (Hong et al., 2024) add length penalties or auxiliary SFT losses.

At the other extreme, reference-free or memory-efficient methods such as CPO (Xu et al., 2024) and SimPO (Meng et al., 2024) remove the reference entirely, improving efficiency and simplifying length normalization, but poten-

tially introducing reward drift. Between these extremes, α -DPO (Wu et al., 2025) interpolates between a fixed SFT model and the evolving policy to form a dynamic reference and reduce distribution shift. Taken together, these works highlight a persistent tension between *stability* (via explicit references) or *flexibility* (via reference-free objectives), motivating methods that can adaptively stabilize preference optimization without inheriting mismatch or inducing drift.

Noise Robustness in Preference Optimization. Real-world preference datasets often contain label noise. Prior work on robust alignment typically emphasizes statistical or distributional treatments of noise. For example, r-DPO (Chowdhury et al., 2024) uses probabilistic label smoothing to reduce the impact of flipped labels, while Dr. DPO (Wu et al., 2024) employs DRO (Duchi & Namkoong, 2019) to account for uncertainty in preference supervision. These methods mainly address noise in the *feedback channel* by modeling label reliability or distributional shift.

An alternative line of robustness is *geometry-aware*: rather than estimating noise rates, one can assess the *local stability* of each preference pair with respect to pessimistic perturbations of the current policy. This perspective suggests that many noisy or spurious signals may be associated with locally brittle instances, motivating instance-wise filtering or reweighting based on local stability.

Relation to Sharpness-Aware Minimization. Our work is conceptually aligned with Sharpness-Aware Minimization (SAM) (Foret et al., 2020), which promotes solutions that lie in flatter neighborhoods to improve generalization. Whereas SAM modifies the update to optimize for global flatness, the same geometric intuition can also inform *instance-wise* robustness in preference learning. In particular, locally pessimistic perturbations can be used to quantify the stability of an implicit preference signal under small distributional shifts. This motivates geometry-aware reweighting schemes that selectively downweight brittle pairs while preserving the underlying preference-optimization update direction, effectively prioritizing locally stable supervision.

3. Preliminaries

We consider the alignment of a policy model π_θ using a pairwise preference dataset $\mathcal{D} = \{(x_i, y_{w,i}, y_{l,i})\}_{i=1}^N$, where $y_{w,i}$ and $y_{l,i}$ denote the preferred and dispreferred responses to prompt x_i , respectively.

Direct Preference Optimization (DPO) DPO (Rafailov et al., 2023) optimizes the policy model by minimizing a logistic (Bradley–Terry) loss over pairwise preferences. It uses a fixed reference model π_{ref} (typically the SFT model)

$$\mathcal{L}_{\text{DPO}}(\theta) = -\mathbb{E}_{(x, y_w, y_l) \sim \mathcal{D}} \left[\log \sigma \left(\beta \log \frac{\pi_\theta(y_w|x)}{\pi_{\text{ref}}(y_w|x)} - \beta \log \frac{\pi_\theta(y_l|x)}{\pi_{\text{ref}}(y_l|x)} \right) \right]$$

$$\mathcal{L}_{\text{SimPO}}(\theta) = -\mathbb{E}_{(x, y_w, y_l) \sim \mathcal{D}} \left[\log \sigma \left(\left(\frac{\beta}{|y_w|} \log \pi_\theta(y_w|x) - \frac{\beta}{|y_l|} \log \pi_\theta(y_l|x) \right) - \gamma \right) \right]$$

$$\mathcal{L}_{\text{GAPO}}(\theta) = -\mathbb{E}_{(x, y_w, y_l) \sim \mathcal{D}} \left[\log \sigma \left(\frac{\beta}{|y_w|} \log \frac{\pi_\theta(y_w|x)}{\pi_{\theta+\epsilon}(y_w|x)} - \frac{\beta}{|y_l|} \log \frac{\pi_\theta(y_l|x)}{\pi_{\theta+\epsilon}(y_l|x)} \right) \right]$$

(a) Objective Functions (Overview)

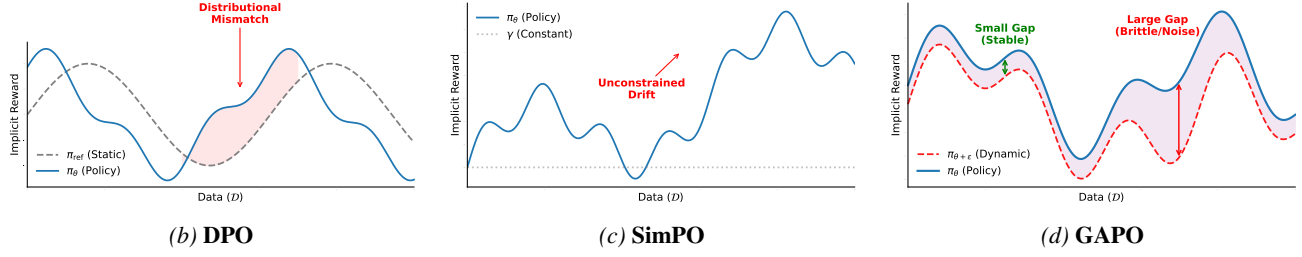


Figure 1. Comparison of Implicit Reward Landscapes and Objectives. (a) Presents the main objective functions. (b-d) Illustrate the reward dynamics of each method. Note that the entire visualization has been rescaled for better fit.

to regularize the deviation of the active policy. The objective is defined as:

$$\mathcal{L}_{\text{DPO}}(\theta) = -\mathbb{E}_{(x, y_w, y_l) \sim \mathcal{D}} \left[\log \sigma \left(\beta \log \frac{\pi_\theta(y_w|x)}{\pi_{\text{ref}}(y_w|x)} - \beta \log \frac{\pi_\theta(y_l|x)}{\pi_{\text{ref}}(y_l|x)} \right) \right], \quad (1)$$

where σ is the sigmoid function and β is an inverse temperature that controls the strength of reference regularization.

Simple Preference Optimization (SimPO) To address the dependency on the reference model and potential length biases, SimPO (Meng et al., 2024) defines a length-normalized reward formulation $p_\theta(x, y) = \frac{1}{|y|} \log \pi_\theta(y|x)$ and introduces a target margin γ . The SimPO objective eliminates π_{ref} as follows

$$\mathcal{L}_{\text{SimPO}}(\theta) = -\mathbb{E}_{(x, y_w, y_l) \sim \mathcal{D}} \left[\log \sigma \left(p_\theta(x, y_w) - p_\theta(x, y_l) - \gamma \right) \right]. \quad (2)$$

Both DPO and SimPO can be viewed as minimizing a logistic loss over the difference of two *implicit rewards*. Specifically, let an implicit reward $r_\theta(x, y)$ be defined such that the objective can be written as $-\log \sigma(r_\theta(x, y_w) - r_\theta(x, y_l))$, up to constants. For DPO, $r_\theta(x, y) = \beta \log \frac{\pi_\theta(y|x)}{\pi_{\text{ref}}(y|x)}$; for SimPO, $r_\theta(x, y) = p_\theta(x, y)$ with margin γ shifting the decision boundary. We will build on this pairwise perspective in the next section.

4. Method

4.1. Geometric Anchor

We adopt the length-normalized implicit reward $p_\theta(x, y)$ (as in SimPO) and define the preference margin for the i -th instance as

$$M_i(\theta) := p_\theta(x_i, y_{w,i}) - p_\theta(x_i, y_{l,i}). \quad (3)$$

We construct a dynamic *geometric anchor* tailored to the local geometry. For each instance i , we seek a perturbation ϵ_i that minimizes the margin $M_i(\theta)$, representing a worst-case scenario within an ℓ_2 ball of radius ρ in parameter space:

$$\epsilon_i^* = \underset{\|\epsilon\|_2 \leq \rho}{\operatorname{argmin}} M_i(\theta + \epsilon). \quad (4)$$

Meanwhile, in stochastic gradient descent, the model parameters evolve along the direction of the *batch-averaged* gradient. To assess stability along this actual optimization trajectory, we employ a batch-wise perturbation strategy. We approximate the worst-case direction using the gradient of the current mini-batch \mathcal{B} :

$$\epsilon_{\mathcal{B}}^* \approx -\rho \frac{\nabla_\theta \left(\frac{1}{|\mathcal{B}|} \sum_{j \in \mathcal{B}} M_j(\theta) \right)}{\left\| \nabla_\theta \left(\frac{1}{|\mathcal{B}|} \sum_{j \in \mathcal{B}} M_j(\theta) \right) \right\|_2}. \quad (5)$$

We then apply this common perturbation to define the anchor parameter $\tilde{\theta} = \theta + \epsilon_{\mathcal{B}}^*$. Using this anchor, we evaluate the anchor margin for each instance i :

$$M_i(\tilde{\theta}) := p_{\tilde{\theta}}(x_i, y_{w,i}) - p_{\tilde{\theta}}(x_i, y_{l,i}). \quad (6)$$

This strategy ensures that the stability verification is aligned with the actual optimization trajectory. By perturbing the model along the collective gradient direction of the batch, we assess whether an instance’s preference signal remains robust under the model’s impending update. To ensure that the anchor acts as a frozen reference, we explicitly apply a *stop-gradient* operator, denoted by $sg(\cdot)$, e.g., $sg(M_i(\theta))$, which returns the same value but blocks gradients from flowing through its argument.

4.2. Objective Function and Anchor Gap

We define the *Anchor Gap* $\Gamma(\theta)$ as the difference between the policy reward function and anchor reward function:

$$\Gamma_i(\theta) := M_i(\theta) - sg(M_i(\tilde{\theta})). \quad (7)$$

We optimize a logistic loss on the anchor gap, which induces instance reweighting that prioritizes samples with small geometric instability:

$$\mathcal{L}_{\text{GAPO}}(\theta) = -\frac{1}{N} \sum_{i=1}^N \log \sigma(\beta \Gamma_i(\theta) - \gamma), \quad (8)$$

where γ is the target margin.

4.3. Optimization Dynamics: Geometric-Aware Reweighting

To understand the optimization mechanism of GAPO, we analyze the gradient of the objective function defined in Eq. (8). Differentiating with respect to θ yields the expected gradient update:

$$\nabla_{\theta} \mathcal{L}(\theta) = -\mathbb{E}_{(x, y_w, y_l) \sim \mathcal{D}} \left[\underbrace{\beta \sigma(\gamma - \beta \Gamma_i(\theta)) \cdot \nabla_{\theta} M_i(\theta)}_{w_i(\theta)} \right] \quad (9)$$

This derivation highlights a key structural property: GAPO preserves the update direction of standard preference optimization ($\nabla_{\theta} M_i(\theta)$) but dynamically scales it by an instance-dependent weight $w_i(\theta) \in (0, \beta)$.

Implicit Geometric Valuation. Unlike static weighting schemes, the weight $w_i(\theta)$ is a function of the instance’s Anchor Gap $\Gamma_i(\theta)$. Since the sigmoid function is monotonically decreasing with respect to the gap, samples with high geometric instability ($\Gamma_i(\theta) \gg 0$) are assigned asymptotically zero weight ($w_i \rightarrow 0$). This confirms that GAPO acts as an automatic *geometric filter*, applying gradients only when the preference signal is structurally stable.

The Resilience-as-Value Hypothesis. We interpret this reweighting mechanism not merely as regularization, but as a dynamic assessment of data value. Our formulation posits that the utility of a preference signal is intrinsically linked to its resilience against local perturbations.

1. **High-Value Data (Resilient \rightarrow High Weight):** Consider an instance i where the preference margin remains robust ($\Gamma_i(\theta) \approx 0$) even under the batch-aligned perturbation. This implies that the preference is grounded in structural, generalized features rather than fragile artifacts. GAPO assigns high weight ($w_i \approx \beta$) to these samples, treating them as the core curriculum for robust alignment.
2. **Low-Value Data (Brittle \rightarrow Low Weight):** Conversely, if the margin collapses under perturbation ($\Gamma_i(\theta) \gg 0$), it indicates that the model’s performance on this instance relied on spurious memorization or incidental parameter correlations. Such brittle signals offer little generalization benefit. GAPO identifies these as low-value instances and suppresses them ($w_i \rightarrow 0$).

5. Theoretical Analysis

In the previous section, we showed that GAPO downweights instances with large Anchor Gaps ($\Gamma_i(\theta)$). Here we provide theoretical support for this mechanism by relating the Anchor Gap to local geometric sensitivity of the preference margin.

5.1. Anchor Gap and Local Geometry

We show that the Anchor Gap upper-bounds a local worst-case degradation of the preference margin, and that (under smoothness) it is controlled by first- and second-order information of M_i .

Theorem 5.1 (Anchor Gap as Local Sharpness). *Consider the ideal worst-case perturbation for an instance i , defined as $\epsilon_i^* = \arg \min_{\|\epsilon\|_2 \leq \rho} M_i(\theta + \epsilon)$. Under the assumption that $M_i(\theta)$ is twice differentiable and ρ is sufficiently small, the Anchor Gap $\Gamma_i(\theta)$ is approximated by:*

$$\Gamma_i(\theta) \leq \rho \|\nabla_{\theta} M_i(\theta)\|_2 - \frac{1}{2} (\epsilon_i^*)^\top \nabla_{\theta}^2 M_i(\theta) \epsilon_i^* + O(\rho^3). \quad (10)$$

Proof. See Appendix A. □

Geometric Interpretation Theorem 5.1 shows that the Anchor Gap provides a tractable proxy for local sensitivity of the margin: large gaps can arise from either a large gradient norm (first-order instability) or high curvature (second-order sensitivity). Rather than directly minimizing sharpness as in SAM, GAPO uses this signal to perform *stability-aware reweighting*. In particular, assigning lower weights to instances with large $\Gamma_i(\theta)$ suppresses locally brittle supervision and biases learning toward preference signals that are stable under small perturbations.

Table 1. Main Results on Instruction-Following Benchmarks. We compare GAPO with various baselines across four models. GAPO consistently outperforms previous methods on AlpacaEval 2.0 and Arena-Hard. **LC**: Length-Controlled, **WR**: Win Rate.

Method	Mistral-Instruct (7B)			Llama-3-Base (8B)		
	AlpacaEval 2		Arena-Hard	AlpacaEval 2		Arena-Hard
	LC (%)	WR (%)	WR (%)	LC (%)	WR (%)	WR (%)
SFT	17.1	14.7	12.6	6.2	4.6	3.3
DPO	26.8	24.9	16.3	18.2	15.5	15.9
IPO	20.3	20.3	16.2	14.4	14.2	17.8
CPO	23.8	28.8	22.6	10.8	8.1	5.8
KTO	24.5	23.6	17.9	14.2	12.4	12.5
ORPO	24.5	24.9	20.8	12.2	10.6	10.8
R-DPO	27.3	24.5	16.1	17.6	14.4	17.2
SimPO	32.1	34.8	21.0	22.0	20.3	23.4
α -DPO	32.3	32.6	21.7	18.3	13.8	22.5
GAPO	35.7	38.7	22.7	22.9	20.6	30.3
Method	Llama-3-Instruct (8B)			Gemma-2-Instruct (9B)		
	AlpacaEval 2		Arena-Hard	AlpacaEval 2		Arena-Hard
	LC (%)	WR (%)	WR (%)	LC (%)	WR (%)	WR (%)
SFT	26.0	25.3	22.3	48.7	36.5	42.1
DPO	40.3	37.9	32.6	70.4	66.9	58.8
IPO	35.6	35.6	30.5	62.6	58.4	53.5
CPO	28.9	32.2	28.8	56.4	53.4	55.2
KTO	33.1	31.8	26.4	61.7	55.5	53.8
ORPO	28.5	27.4	25.8	56.2	46.7	46.2
R-DPO	41.1	37.8	33.1	68.3	66.9	57.9
SimPO	44.7	40.5	33.8	72.4	65.0	57.8
α -DPO	46.6	38.1	33.3	73.4	66.1	60.8
GAPO	47.4	42.8	33.7	74.0	67.7	61.5

Remark While Theorem 5.1 analyzes the ideal instance-specific perturbation ϵ_i^* , our practical implementation employs a batch-shared perturbation ϵ_B^* . This design choice is motivated by the dynamics of stochastic gradient descent: since model parameters evolve along the collective gradient direction of the batch, probing stability along this *actual optimization trajectory* can be more relevant than isolated instance-specific directions. Mathematically, the first-order term in the Anchor Gap becomes the projection $\rho \frac{\nabla M_i^\top \nabla M_B}{\|\nabla M_B\|}$. As a result, optimization is biased toward solutions that are locally more robust.

6. Experiments

In this section, we empirically evaluate GAPO along three complementary dimensions: (1) **General alignment performance** across model families and benchmarks; (2) **R robustness to noisy preferences** under both random and structured noise; and (3) **Geometric data valuation**, examining whether the Anchor Gap is informative for identifying stable

versus brittle supervision.

6.1. Experimental Setup

Models and Datasets. We evaluate GAPO across a representative set of widely-used open(-weight) models. Specifically, we utilize Mistral-Instruct-v0.2 (7B) (Jiang et al., 2023), Llama-3-Base/Instruct (8B) (AI@Meta, 2024), and Gemma-2-Instruct (9B) (Team et al., 2024) as our backbone models. For the main alignment experiments, we follow the standard protocol of SimPO (Meng et al., 2024) and train on the UltraFeedback dataset (Cui et al., 2023). To evaluate robustness under noisy preferences, we follow the experimental protocol of Dr. DPO (Wu et al., 2024). We train Pythia-2.8B (Biderman et al., 2023) on the Anthropic HH dataset (Bai et al., 2022) and inject synthetic pairwise noise by flipping preference labels at varying rates.

Baselines. We compare GAPO against a comprehensive suite of offline alignment methods, covering both reference-based and reference-free paradigms: DPO (Rafailov et al.,

Table 2. Reasoning vs. Alignment Trade-off across Models
Performance comparison on Mistral-Instruct and Llama-3-Base.

Model	Method	AlpacaEval 2	GSM8k	ARC-C
Mistral-7B	DPO	26.8	41.8	66.7
	RDPO	27.3	42.6	67.5
	SimPO	32.1	36.6	66.3
	α -DPO	32.3	29.3	65.2
	GAPO	35.7	40.3	66.3
Llama-3-8B	DPO	18.2	55.5	65.6
	RDPO	17.6	54.9	65.2
	SimPO	22.0	53.0	65.2
	α -DPO	18.3	45.4	66.0
	GAPO	22.9	56.0	67.2

Table 3. Robustness against label noise. Comparison under random and length-dependent flipping. In both settings, GAPO shows superior resilience compared to baselines.

Flip	Method	0%	10%	20%	30%	40%
Random	DPO	63.3	62.3	62.9	58.5	57.0
	Dr.DPO	66.2	65.4	64.2	62.7	58.8
	GAPO	66.8	65.6	64.9	62.8	59.8
Length-dependent	DPO	63.3	51.7	54.3	54.3	52.0
	Dr.DPO	66.2	62.1	49.2	48.3	44.9
	GAPO	66.8	63.3	58.3	56.6	52.0

2023), IPO (Azar et al., 2024), KTO (Ethayarajh et al., 2024), CPO (Xu et al., 2024), ORPO (Hong et al., 2024), R-DPO (Park et al., 2024), SimPO (Meng et al., 2024) and α -DPO (Wu et al., 2025).

Evaluation Metrics. We assess instruction-following capability using AlpacaEval 2.0 (Li et al., 2023) and Arena-Hard v0.1 (Li et al., 2024), which correlate highly with human judgement. To evaluate the impact on general reasoning capabilities (the “alignment tax”), we report performance on standard benchmarks including GSM8k (Cobbe et al., 2021) and ARC-C (Clark et al., 2018).

6.2. Main Results

Alignment Performance. Table 1 summarizes instruction-following performance across model families. Overall, GAPO is consistently competitive and typically improves alignment metrics relative to strong reference-based and reference-free baselines. The gains are not confined to a single benchmark: we observe improvements on both AlpacaEval 2.0 and Arena-Hard, suggesting that the benefit is not merely an artifact of a particular evaluator.

Reasoning Preservation. A common pitfall of preference optimization is the trade-off between improved instruction-

Table 4. Data Efficiency & valuation. Comparison of SimPO models trained on 30% data subsets selected by the Anchor Gap (Γ). The Stable subset outperforms Random and Unstable.

Sampling (30%)	Metric	AlpacaEval2	GSM8k	ARC-C
Random	-	12.8	54.3	63.6
Unstable	High Γ	9.80	54.8	63.4
Stable	Low Γ	13.8	56.2	64.2

following and degraded reasoning (the *alignment tax*). Table 2 shows that GAPO improves alignment while largely preserving reasoning performance across model families. In particular, compared to reference-free training that can exhibit drift, GAPO tends to maintain stronger reasoning scores while still delivering alignment gains.

Robustness Against Label Noise. We evaluate robustness under both random label flips and a more structured noise setting that selectively flips pairs based on response length (creating a “shorter is better” bias). We report Reward Accuracy on the test set. Table 3 shows that robust baselines mitigate performance degradation as noise increases, and GAPO remains among the most resilient methods across noise rates and noise types. This supports the view that instance-wise reweighting can suppress the influence of brittle or noisy preference pairs without explicitly estimating noise rates.

Geometric Data Valuation. To evaluate whether the Anchor Gap Γ is informative about supervision quality, we conduct a data pruning experiment. We sort the training instances by Γ and construct three subsets (each 30% of the data): (1) Stable Subset (Lowest Γ): representing geometrically robust instances; (2) Unstable Subset (Highest Γ): representing brittle ; and (3) Random Subset: serving as a baseline. To avoid circularity (i.e., pruning with GAPO and then re-training GAPO on the pruned data), we train a fixed reference-free learner (SimPO) on each subset under identical hyperparameters. This isolates the effect of Anchor-Gap-based selection and evaluates whether the induced data ranking generalizes beyond GAPO itself.

Table 4 shows a clear ranking: training on the Stable subset yields the best performance, Random is intermediate, and Unstable subset is the weakest. This suggests that instances with large Anchor Gaps are detrimental to alignment (negative transfer), likely due to noise or spurious correlations. More broadly, this supports the view that instance-wise reweighting can act as an implicit data curation mechanism by emphasizing stable preference signals.

6.3. Geometric Analysis: Hessian Eigenspectrum

To complement the theoretical analysis, we measure the local curvature of models trained with DPO, SimPO, and

Table 5. Hessian Eigenspectrum Analysis. Comparison of the Hessian eigenvalues (λ) averaged over 1,000 samples from the training set.

Method	λ_{max} (Sharpness) \downarrow	Top-5 Avg \downarrow	λ_{min}
DPO	149.6	103.4	-143.1
SimPO	158.8	98.9	-106.9
GAPO	145.1	94.9	-81.4

GAPO by approximating the Hessian eigenspectrum via the Lanczos algorithm, reporting eigenvalues (λ) averaged over training batches. To reduce computational cost, we estimate the eigenspectrum only for the final projection (LM head) parameters; thus, these results should be interpreted as a targeted probe of local sharpness rather than a full-model curvature estimate.

Sharpness. Table 5 compares the Hessian eigenvalues. Large positive eigenvalues (e.g., λ_{max}) indicate sharp directions, which are often associated with worse generalization (Foret et al., 2020; Keskar et al., 2017). Across methods, GAPO exhibits a small λ_{max} in this analysis, consistent with reduced sharpness in the probed subspace.

Subspace curvature profile. The trend is also reflected in the top-eigenvalue averages. While this does not by itself establish global flatness, it provides empirical support that the geometry-aware reweighting of GAPO can bias optimization toward locally less sharp solutions.

Notably, the Hessian is often indefinite, exhibiting both positive and negative curvature (Dauphin et al., 2014), a characteristic feature of saddle points. Under a second-order approximation, the magnitude of the most negative eigenvalue $|\lambda_{min}|$ characterizes the steepness of the locally most unstable direction. Compared to DPO/SimPO, GAPO exhibits a substantially smaller-magnitude negative curvature, suggesting reduced local instability in the LM-head subspace. This suggests that while the solution remains a saddle point, GAPO locates a region with significantly reduced local instability, making the policy robust.

6.4. Ablation Studies

We study key design choices of GAPO, focusing on the perturbation strategy, radius, and scope. Unless otherwise specified, all ablations are evaluated on AlpacaEval 2.0.

Table 6. Effect of Calculation Strategy. Comparison between instance-specific and batch-shared perturbation directions.

Strategy	AlpacaEval2	Arena-Hard
Instance-wise	33.7	23.4
Batch-wise	35.7	22.7

Batch-wise vs. Instance-wise Perturbation. We first study how the perturbation direction is computed. Table 6 shows that batch-wise perturbation yields stronger AlpacaEval 2.0 performance, while the instance-wise variant can slightly improve Arena-Hard.

A plausible explanation is *trajectory-consistent probing*: since updates follow the batch-averaged gradient, batch-shared perturbations probe instability along the same direction the optimizer is likely to move. In contrast, per-instance perturbations can be heterogeneous and may not align with the effective update direction, producing noisier anchor gaps.

Table 7. Effect of Perturbation Radius (ρ). Performance sensitivity across different perturbation magnitudes on Mistral-Instruct and Llama-3-Base.

Radius (ρ)	Mistral-Instruct	Llama-3-Base
0.025	37.9	20.8
0.05	38.7	22.9
0.075	37.3	20.5
0.10	37.0	20.2

Sensitivity to Perturbation Radius (ρ) Table 7 examines the effect of perturbation magnitude. If ρ is too small the anchor may not sufficiently stress-test local geometry; if too large ($\rho \geq 0.075$), the anchor may move beyond a trusted neighborhood and introduce additional noise. Overall, $\rho = 0.05$ provides a favorable balance between sensitivity and stability.

Table 8. Effect of Perturbation Scope. Comparison between perturbing only the last layer versus full parameters.

Scope	Score
LM head	20.7
Full Parameters	22.9

Perturbation Scope Table 8 compares perturbing only the last layer (LM head) versus the full model. Full-parameter perturbation yields better performance, suggesting that preference overfitting and geometric brittleness are not confined to the final projection but reflect properties of the broader representation.

6.5. Distinguishing GAPO from Sharpness-Aware Minimization

Since GAPO is motivated by local geometry, a natural question is whether its gains can be explained solely by *flatness-seeking optimization*. To probe this, we compare GAPO against SimPO trained with the SAM opti-

Table 9. Effectiveness of Geometric Reweighting. Comparison between standard optimization (SimPO), blindly seeking flatness (SimPO+SAM), and our geometric valuation strategy (GAPO) on Mistral-7B. GAPO significantly outperforms the direct SAM application.

Method	AlpacaEval 2	Arena-Hard	GSM8k	ARC-C
SimPO	32.1	21.0	36.6	66.3
SimPO+SAM	34.9	20.1	38.6	66.1
GAPO	35.7	22.7	40.3	66.3

mizer (SimPO+SAM), using the same perturbation radius $\rho = 0.05$ on Mistral-7B.

Table 9 suggests that SAM can provide modest improvements over standard SimPO on some metrics, but the effect is not uniformly positive across evaluators. In contrast, GAPO tends to deliver more consistent gains across instruction-following and reasoning metrics in this setting.

These observations indicate that GAPO is not simply an optimizer-level flatness trick. SAM promotes *global* flatness by perturbing parameters during optimization and applying the same geometric bias to all training pairs. GAPO instead uses the *anchor gap* as an explicit per-example geometric signal and converts it into *instance-wise reweighting* within a DPO/SimPO-style objective. Empirically, this targeted reweighting appears to be a more effective use of local geometry for preference optimization.

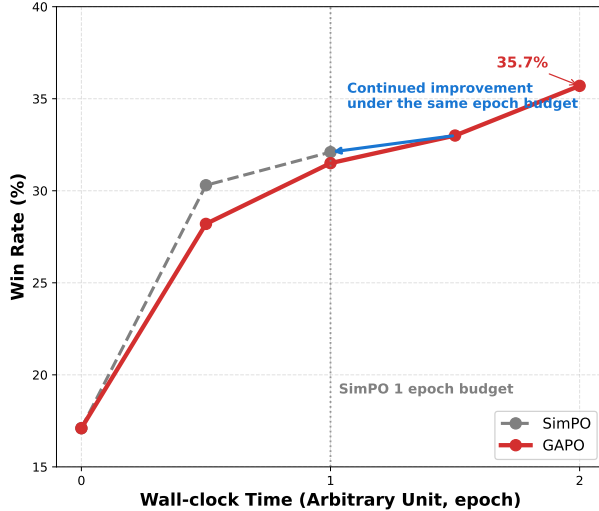


Figure 2. Wall-clock training dynamics on Mistral-7B. All methods are trained for a single epoch. GAPO continues to improve during later optimization stages, while SimPO saturates after its standard training regime.

6.6. Computational Efficiency vs Convergence Quality

A practical consideration is the additional overhead of constructing the geometric anchor, which increases wall-clock

time per optimization step by roughly $\sim 2\times$ compared to SimPO. To account for this, we analyze training progress as a function of wall-clock time (Figure 2). Overall, GAPO exhibits competitive time-efficiency: despite the higher per-step cost, it reaches performance comparable to SimPO within a similar time budget and can continue improving beyond the point where baseline methods saturate. This suggests that the extra computation is not merely overhead, but can translate into improved final performance when additional training time is available.

7. Conclusion

We presented **Geometric Anchor Preference Optimization (GAPO)**, a geometry-aware framework for offline preference optimization that stabilizes learning without relying on a fixed reference. The key idea is to construct a pessimistic local anchor around the current policy and use the resulting *Anchor Gap* as an instance-wise signal to reweight pairwise preference updates, suppressing locally brittle supervision while emphasizing stable preference signals.

On the theory side, we related the Anchor Gap to local geometric sensitivity of the preference margin, providing support for stability-aware reweighting. Empirically, GAPO improves alignment performance across model families while maintaining reasoning ability, and it remains resilient under both random and structured preference noise. Beyond optimization, our results suggest a broader insight: local geometric stability can serve as a practical proxy for the reliability of preference supervision, enabling preference learning methods to act as implicit data curators

Impact Statement

This paper introduces Geometric Anchor Preference Optimization (GAPO), a preference-based alignment method that downweights brittle preference pairs by measuring the stability of margins under small local perturbations. GAPO may improve robustness to noisy or inconsistent human feedback and help preserve general capabilities during alignment, which could benefit practical LLM deployment where preference data is imperfect.

However, GAPO does not guarantee safety, fairness, or truthfulness, and it may still amplify biases or harmful patterns present in the preference data. The method can also introduce additional computational overhead compared to standard preference optimization. We recommend pairing GAPO with careful data curation and broader safety evaluations when training and deploying aligned models.

References

- AI@Meta. Llama 3 model card. 2024. URL https://github.com/meta-llama/llama3/blob/main/MODEL_CARD.md.
- Azar, M. G., Guo, Z. D., Piot, B., Munos, R., Rowland, M., Valko, M., and Calandriello, D. A general theoretical paradigm to understand learning from human preferences. In *International Conference on Artificial Intelligence and Statistics*, pp. 4447–4455. PMLR, 2024.
- Bai, Y., Jones, A., Ndousse, K., Askell, A., Chen, A., Das-Sarma, N., Drain, D., Fort, S., Ganguli, D., Henighan, T., et al. Training a helpful and harmless assistant with reinforcement learning from human feedback. *arXiv preprint arXiv:2204.05862*, 2022.
- Biderman, S., Schoelkopf, H., Anthony, Q. G., Bradley, H., O’Brien, K., Hallahan, E., Khan, M. A., Purohit, S., Prashanth, U. S., Raff, E., et al. Pythia: A suite for analyzing large language models across training and scaling. In *International Conference on Machine Learning*, pp. 2397–2430. PMLR, 2023.
- Chowdhury, S. R., Kini, A., and Natarajan, N. Provably robust dpo: Aligning language models with noisy feedback. *arXiv preprint arXiv:2403.00409*, 2024.
- Christian, P. F., Leike, J., Brown, T., Martic, M., Legg, S., and Amodei, D. Deep reinforcement learning from human preferences. *Advances in neural information processing systems*, 30, 2017.
- Clark, P., Cowhey, I., Etzioni, O., Khot, T., Sabharwal, A., Schoenick, C., and Tafjord, O. Think you have solved question answering? try arc, the ai2 reasoning challenge, 2018. URL <https://arxiv.org/abs/1803.05457>.
- Cobbe, K., Kosaraju, V., Bavarian, M., Chen, M., Jun, H., Kaiser, L., Plappert, M., Tworek, J., Hilton, J., Nakano, R., Hesse, C., and Schulman, J. Training verifiers to solve math word problems, 2021. URL <https://arxiv.org/abs/2110.14168>.
- Cui, G., Yuan, L., Ding, N., Yao, G., Zhu, W., Ni, Y., Xie, G., Liu, Z., and Sun, M. Ultrafeedback: Boosting language models with high-quality feedback. 2023.
- Dauphin, Y., Pascanu, R., Gulcehre, C., Cho, K., Ganguli, S., and Bengio, Y. Identifying and attacking the saddle point problem in high-dimensional non-convex optimization, 2014. URL <https://arxiv.org/abs/1406.2572>.
- Duchi, J. and Namkoong, H. Variance-based regularization with convex objectives. *Journal of Machine Learning Research*, 20(68):1–55, 2019.
- Ethayarajh, K., Xu, W., Muennighoff, N., Jurafsky, D., and Kiela, D. Kto: Model alignment as prospect theoretic optimization. *arXiv preprint arXiv:2402.01306*, 2024.
- Foret, P., Kleiner, A., Mobahi, H., and Neyshabur, B. Sharpness-aware minimization for efficiently improving generalization. *arXiv preprint arXiv:2010.01412*, 2020.
- Hong, J., Lee, N., and Thorne, J. Orpo: Monolithic preference optimization without reference model. *arXiv preprint arXiv:2403.07691*, 2024.
- Jiang, D., Liu, Y., Liu, S., Zhao, J., Zhang, H., Gao, Z., Zhang, X., Li, J., and Xiong, H. From clip to dino: Visual encoders shout in multi-modal large language models. *arXiv preprint arXiv:2310.08825*, 2023.
- Keskar, N. S., Mudigere, D., Nocedal, J., Smelyanskiy, M., and Tang, P. T. P. On large-batch training for deep learning: Generalization gap and sharp minima. In *International Conference on Learning Representations*, 2017. URL <https://openreview.net/forum?id=H1oyR1Ygg>.
- Li, T., Chiang, W.-L., Frick, E., Dunlap, L., Zhu, B., Gonzalez, J. E., and Stoica, I. From live data to high-quality benchmarks: The arena-hard pipeline, April 2024. URL <https://lmsys.org/blog/2024-04-19-arena-hard/>.
- Li, X., Zhang, T., Dubois, Y., Taori, R., Gulrajani, I., Guestrin, C., Liang, P., and Hashimoto, T. B. Alpacaeval: An automatic evaluator of instruction-following models. https://github.com/tatsu-lab/alpaca_eval, 5 2023.
- Lin, Y., Lin, H., Xiong, W., Diao, S., Liu, J., Zhang, J., Pan, R., Wang, H., Hu, W., Zhang, H., et al. Mitigating the alignment tax of rlhf. In *Proceedings of the 2024 Conference on Empirical Methods in Natural Language Processing*, pp. 580–606, 2024.
- Meng, Y., Xia, M., and Chen, D. Simpo: Simple preference optimization with a reference-free reward. *Advances in Neural Information Processing Systems*, 37:124198–124235, 2024.
- Noukhovitch, M., Lavoie, S., Strub, F., and Courville, A. C. Language model alignment with elastic reset. *Advances in Neural Information Processing Systems*, 36:3439–3461, 2023.
- Ouyang, L., Wu, J., Jiang, X., Almeida, D., Wainwright, C., Mishkin, P., Zhang, C., Agarwal, S., Slama, K., Ray, A., et al. Training language models to follow instructions with human feedback. *Advances in neural information processing systems*, 35:27730–27744, 2022.

Park, R., Rafailov, R., Ermon, S., and Finn, C. Disentangling length from quality in direct preference optimization. *arXiv preprint arXiv:2403.19159*, 2024.

Rafailov, R., Sharma, A., Mitchell, E., Manning, C. D., Ermon, S., and Finn, C. Direct preference optimization: Your language model is secretly a reward model. *Advances in neural information processing systems*, 36: 53728–53741, 2023.

Schulman, J., Wolski, F., Dhariwal, P., Radford, A., and Klimov, O. Proximal policy optimization algorithms. *arXiv preprint arXiv:1707.06347*, 2017.

Team, G., Riviere, M., Pathak, S., Sessa, P. G., Hardin, C., Bhupatiraju, S., Hussenot, L., Mesnard, T., Shahriari, B., Ramé, A., et al. Gemma 2: Improving open language models at a practical size. *arXiv preprint arXiv:2408.00118*, 2024.

Wu, J., Xie, Y., Yang, Z., Wu, J., Chen, J., Gao, J., Ding, B., Wang, X., and He, X. Towards robust alignment of language models: Distributionally robustifying direct preference optimization. *arXiv preprint arXiv:2407.07880*, 2024.

Wu, J., Wang, X., Yang, Z., Wu, J., Gao, J., Ding, B., Wang, X., and He, X. AlphaDPO: Adaptive reward margin for direct preference optimization. In *Forty-second International Conference on Machine Learning*, 2025. URL <https://openreview.net/forum?id=ETLKYVMVLt>.

Xiong, W., Dong, H., Ye, C., Wang, Z., Zhong, H., Ji, H., Jiang, N., and Zhang, T. Iterative preference learning from human feedback: Bridging theory and practice for RLHF under KL-constraint. In Salakhutdinov, R., Kolter, Z., Heller, K., Weller, A., Oliver, N., Scarlett, J., and Berkenkamp, F. (eds.), *Proceedings of the 41st International Conference on Machine Learning*, volume 235 of *Proceedings of Machine Learning Research*, pp. 54715–54754. PMLR, 21–27 Jul 2024. URL <https://proceedings.mlr.press/v235/xiong24a.html>.

Xu, H., Sharaf, A., Chen, Y., Tan, W., Shen, L., Van Durme, B., Murray, K., and Kim, Y. J. Contrastive preference optimization: Pushing the boundaries of llm performance in machine translation. *arXiv preprint arXiv:2401.08417*, 2024.

A. Theoretical Derivations

In this section, we provide detailed derivations of the gradient update rule for GAPO and a proof of Theorem 5.1, which connects the Anchor Gap to local geometric sharpness.

A.1. Derivation of GAPO Gradient Update Rule

Recall the GAPO objective function defined in Eq. (9):

$$\mathcal{L}(\theta) = -\frac{1}{N} \sum_{i=1}^N \log \sigma(\beta \Gamma_i(\theta) - \gamma), \quad (11)$$

where the Anchor Gap is $\Gamma_i(\theta) = M_i(\theta) - \text{sg}(M_i(\tilde{\theta}))$. Note that the anchor term $M_i(\tilde{\theta})$ is treated as a constant (stop-gradient) during the update step.

Let $z_i = \beta \Gamma_i(\theta) - \gamma$. The gradient with respect to θ is:

$$\nabla_{\theta} \mathcal{L}(\theta) = -\frac{1}{N} \sum_{i=1}^N \frac{\partial}{\partial \theta} \log \sigma(z_i) \quad (12)$$

$$= -\frac{1}{N} \sum_{i=1}^N (1 - \sigma(z_i)) \frac{\partial z_i}{\partial \theta} \quad (13)$$

$$= -\frac{1}{N} \sum_{i=1}^N \sigma(-z_i) \cdot \beta \nabla_{\theta} \Gamma_i(\theta). \quad (14)$$

Since $\nabla_{\theta} \Gamma_i(\theta) = \nabla_{\theta} M_i(\theta)$, we substitute z_i :

$$\nabla_{\theta} \mathcal{L}(\theta) = -\frac{1}{N} \sum_{i=1}^N [\beta \sigma(-(\beta \Gamma_i(\theta) - \gamma))] \nabla_{\theta} M_i(\theta). \quad (15)$$

By defining the instance-dependent weight as $w_i(\theta) = \beta \sigma(\gamma - \beta \Gamma_i(\theta))$, we recover Eq. (12) from the main text:

$$\nabla_{\theta} \mathcal{L}(\theta) = -\mathbb{E}_{\mathcal{D}} [w_i(\theta) \cdot \nabla_{\theta} M_i(\theta)]. \quad (16)$$

This confirms that GAPO performs weighted margin maximization, where the weight w_i decays as the instability gap Γ_i increases.

A.2. Proof of Theorem 5.1

Proof. The Anchor Gap is defined as the discrepancy between the current reward and the reward under the worst-case perturbation:

$$\Gamma_i(\theta) := M_i(\theta) - M_i(\theta + \epsilon_i^*) \quad (17)$$

Performing a second-order Taylor expansion of $M_i(\theta + \epsilon_i^*)$ around θ :

$$M_i(\theta + \epsilon_i^*) = M_i(\theta) + \nabla_{\theta} M_i(\theta)^{\top} \epsilon_i^* + \frac{1}{2} (\epsilon_i^*)^{\top} \nabla_{\theta}^2 M_i(\theta) \epsilon_i^* + O(\rho^3) \quad (18)$$

Substituting this back into the definition of $\Gamma_i(\theta)$, we obtain:

$$\Gamma_i(\theta) = -\nabla_{\theta} M_i(\theta)^{\top} \epsilon_i^* - \frac{1}{2} (\epsilon_i^*)^{\top} \nabla_{\theta}^2 M_i(\theta) \epsilon_i^* + O(\rho^3) \quad (19)$$

To determine the optimal perturbation ϵ_i^* , we solve the minimization problem $\min_{\|\epsilon\| \leq \rho} M_i(\theta + \epsilon)$. Since ρ is small, the first-order term dominates the local change. To minimize the inner product $\nabla_{\theta} M_i(\theta)^{\top} \epsilon$, the vector ϵ must be aligned opposite to the gradient $\nabla_{\theta} M_i(\theta)$. Thus, the optimal first-order perturbation is:

$$\epsilon_i^* \approx -\rho \frac{\nabla_{\theta} M_i(\theta)}{\|\nabla_{\theta} M_i(\theta)\|_2} \quad (20)$$

Substituting this result into the first term of Eq. (19):

$$-\nabla_{\theta} M_i(\theta)^{\top} \epsilon_i^* \approx -\nabla_{\theta} M_i(\theta)^{\top} \left(-\rho \frac{\nabla_{\theta} M_i(\theta)}{\|\nabla_{\theta} M_i(\theta)\|_2} \right) \quad (21)$$

$$= \rho \frac{\|\nabla_{\theta} M_i(\theta)\|_2^2}{\|\nabla_{\theta} M_i(\theta)\|_2} \quad (22)$$

$$= \rho \|\nabla_{\theta} M_i(\theta)\|_2 \quad (23)$$

Replacing the first term in Eq. (19), we arrive at:

$$\Gamma_i(\theta) \approx \rho \|\nabla_{\theta} M_i(\theta)\|_2 - \frac{1}{2} (\epsilon_i^*)^{\top} \nabla_{\theta}^2 M_i(\theta) \epsilon_i^* \quad (24)$$

Geometric Interpretation:

- The first term $\rho \|\nabla_{\theta} M_i(\theta)\|_2$ represents the slope of the reward landscape. A smaller norm indicates a flatter region (local extremum).
- The second term involves the Hessian $H_i = \nabla_{\theta}^2 M_i(\theta)$. Since we maximize the reward margin M_i , the function is locally concave around a maximum, implying H_i is negative semi-definite ($\epsilon^{\top} H_i \epsilon \leq 0$). Consequently, the term $-\frac{1}{2} \epsilon^{\top} H_i \epsilon$ becomes non-negative. This acts as a penalty for sharpness: the more curved (sharp) the peak, the larger the Anchor Gap.

Thus, minimizing $\Gamma_i(\theta)$ is theoretically equivalent to seeking flat minima by minimizing both the gradient norm and the curvature. \square

B. Implementation Details

B.1. Hyperparameters

We provide the detailed hyperparameters used for training GAPO and baselines across all models in Table 10, following the SimPO setting (Meng et al., 2024). We utilized $4 \times$ B200 GPUs for training the 7B/8B/9B models.

Table 10. Hyperparameters for GAPO and baselines.

Hyperparameter	Mistral-7B Instruct	Llama-3-8B Base	Llama-3-8B Instruct	Gemma-2-9B
Learning Rate	5e-7	6e-7	1e-6	8e-7
Global Batch Size	128	128	128	128
LR Scheduler	Cosine	Cosine	Cosine	Cosine
Warmup Ratio	0.1	0.1	0.1	0.1
Max Length	2048	2048	2048	2048
GAPO Specifics				
Beta (β)	2.5	2.0	2.5	10
Gamma (γ)	0.1	0.5	0.55	0.5
Perturbation ρ	0.05	0.05	0.05	0.05
Anchor Update	Batch-wise	Batch-wise	Batch-wise	Batch-wise

C. Computational Efficiency Analysis

In this section, we provide a detailed breakdown of the computational cost and training dynamics. Generating the pessimistic anchor in GAPO requires an additional forward-backward pass per optimization step, resulting in roughly $\sim 2 \times$ wall-clock time compared to standard SimPO. To evaluate whether this overhead is justified, Figure 2 compares the training trajectories normalized by GPU hours:

- **Initial Efficiency (1.5 Hours):** At the 1.5-hour mark, SimPO completes 1 full epoch, while GAPO completes approximately 0.5 epochs. Despite the fewer update steps, GAPO achieves a performance level *comparable* to SimPO.
- **Long-term Convergence:** As training progresses beyond this point, SimPO’s performance gains tend to diminish or saturate. In contrast, GAPO effectively leverages the extended training time to further refine the policy, ultimately achieving a significantly higher convergence ceiling.

This analysis confirms that while GAPO has a higher upfront cost per step, it is a more effective strategy for maximizing final model performance, effectively trading compute time for robustness and alignment quality.

D. Qualitative Analysis: Geometric Data Valuation

We provide additional qualitative examples to illustrate how GAPO identifies and handles different types of data quality issues. Table 11 showcases a *Safety/Robustness Failure* case (Unstable) and a *Robust Reasoning* case (Stable) with a detailed answer.

Table 11. Extended Qualitative Analysis. **Case A (Unstable)** shows the model failing to robustly reject corrupted text (near-zero margin), which GAPO flags via a large Anchor Gap. **Case B (Stable)** illustrates a robust logical refusal, where the preference for the high-quality response is geometrically strengthened.

Case A: Unstable Geometry (Susceptibility to Token Noise)	
Prompt	[INST] Can you provide a new sentence using synonyms for the words "fresh" and "tasty" to describe the produce? [/INST]
Model Output	Chosen: "Upon encountering the market’s offerings, I was struck by the vibrant, uncooked produce..." Rejected: "Absolutely. How about "The market’s vibrant offerings showcase ... <i>t*****/easel** produce**</i> , with ... <i>t***** flavors...</i> ""
Metrics	Anchor Gap (Γ): +3.24 (High Instability) Original Margin (M): +0.05 (Model Confused/Uncertain)
Diagnosis	Safety & Robustness Failure. The Rejected response contains severe token corruption and noise. Alarmingly, the original model is ambivalent ($M \approx 0$), barely preferring the clean text over the corrupted one. The large Anchor Gap reveals this fragility: under perturbation, the model’s preference shifts drastically. GAPO correctly identifies this instance as unreliable and downweights it to prevent learning from such noisy decision boundaries.
Case B: Stable Geometry (Robust Logic)	
Prompt	[INST] If 96 people want to take a boat trip in 10 days, then how many will it take? [/INST]
Model Output	Chosen: "The information provided in the question is not sufficient to determine how many people can take the boat trip each day... Assuming there is a boat with a capacity for 96 people..." Rejected: "The information provided in the question is not sufficient... The question states that 96 people in total want to take the trip, but it does not specify how the 10 days relate to the number of people taking the trip each day. It could be that 96 people take the trip once, or that 16 people take the trip twice... Without more information, it is impossible to determine..."
Metrics	Anchor Gap (Γ): -1.79 (High Stability) Original Margin (M): +0.81 (Moderate Confidence)
Diagnosis	Deep Semantic Stability. Both responses correctly identify the logical flaw in the prompt (trick question). However, the model maintains a stable preference for the Chosen response (likely due to better structure or phrasing). The negative Anchor Gap ($\Gamma < 0$) indicates that this preference is not brittle; even when the model parameters are perturbed to minimize the margin, the model defends its choice. GAPO treats this as a core, high-quality alignment signal.

Prompt/Instruction

When was Canada colonized?

SimPO

Canada was not strictly colonized in the same way that European countries established colonies... Instead, it developed as a series of British territories, starting with the founding of the first permanent European settlement at Cabot Tower in present-day Nova Scotia in 1597, and continuing with the establishment of New France (Quebec) in 1608. [...]

Analysis: The model hallucinates a non-existent settlement date (1597) and location (Cabot Tower was built in 1897).

GAPO

Canada was not strictly colonized... Instead, it developed as a series of British territories, starting with the founding of the first permanent European settlement at Cabot Strait in 1497 (believed to be by John Cabot...), and continuing with the establishment of New France (1608)... British rule was formally established... following the Treaty of Paris in 1763. [...]

Analysis: The model correctly identifies the historical date (1497) and key events like the Treaty of Paris.

Figure 3. Comparison of model outputs on historical facts. The loser model (left) generates a hallucination regarding the first settlement date and location (1597 vs. 1497), whereas the winner model (right) provides historically accurate details.

D.1. Qualitative Analysis: Mitigating Hallucinations via Geometric Anchoring

To provide a concrete understanding of how GAPO improves generation quality compared to unconstrained baselines, we conduct a qualitative case study on historical fact retrieval. Figure 3 illustrates a comparison between SimPO and GAPO given the prompt: “*When was Canada colonized?*”

Unconstrained Drift and Hallucination (SimPO). The response generated by SimPO (left in Figure 3) exhibits a characteristic failure mode of unconstrained preference optimization. While the text is fluent and structurally coherent, it suffers from severe **factual hallucinations**. Specifically, the model fabricates a settlement date (“1597”) and incorrectly identifies “Cabot Tower” (actually built in 1897) as a 16th-century settlement. This aligns with our hypothesis that without a stabilizing anchor, the model may drift into regions of the parameter space that maximize the implicit reward (e.g., style, length) at the expense of factual integrity.

Factual Grounding via Stability (GAPO). In contrast, GAPO (right) produces a historically accurate response. It correctly identifies the landing of John Cabot in 1497 (Cabot Strait) and references key historical milestones such as the establishment of New France (1608) and the Treaty of Paris (1763). From a geometric perspective, factual knowledge typically resides in more stable regions of the loss landscape compared to hallucinations, which are often “sharp” artifacts of overfitting. By penalizing geometric instability via the Anchor Gap, GAPO effectively filters out these brittle hallucinations, forcing the model to rely on robust, generalized knowledge representations. This case study suggests that geometric anchoring not only improves scalar metrics but also enhances the trustworthiness of the generated content.

D.2. GAPO Pseudo-code

Algorithm 1 illustrates the PyTorch-style implementation of the Geometric Anchor construction and loss calculation.

Algorithm 1 GAPO Pseudo-code

```
def gapo_loss(model, batch, beta, gamma, rho):
    # 1. Forward Pass & Margin calculation
    logps_w, logps_l = get_log_probs(model, batch)
    margin = (logps_w - logps_l).mean()

    # 2. Compute Adversarial Perturbation
    grads = torch.autograd.grad(-margin, model.parameters())
    gnorm = torch.norm(torch.stack([g.norm() for g in grads]))
    eps = {p: -rho * (g / (gnorm + 1e-8)) for p, g in zip(model.parameters(), grads)}

    # 3. Apply Perturbation & Compute Anchor Margin
    with torch.no_grad():
        for p in model.parameters(): p.add_(eps[p])
        anchor_w, anchor_l = get_log_probs(model, batch)
        m_anchor = (anchor_w - anchor_l).detach()
        for p in model.parameters(): p.sub_(eps[p]) # Restore

    # 4. Compute GAPO Loss
    gap = (logps_w - logps_l) - m_anchor
    return -F.logsigmoid(beta * gap - gamma).mean()
```
